Int J Adv Manuf Technol (2017) 90:349–359
DOI 10.1007/s00170-016-9387-5

ORIGINAL ARTICLE

# An analytical modeling for springback prediction during U-bending process of advanced high-strength steels based on anisotropic nonlinear kinematic hardening model

**Asghar. Zajkani**[1] · **Hamid Hajbarati**[1]

Received: 11 March 2016 / Accepted: 24 August 2016 / Published online: 1 September 2016


**Abstract** An undesirable factor that affects the dimensional precision and final shape of metallic parts produced in cold forming processes is springback phenomenon. In this paper, an analytical model is introduced to predict springback in U-shaped bending process of DP780 dual-phase steel sheet. It is based on the Hill48 yielding criterion and plane strain condition. In this model, the effect of forming history, the sheet thinning, and the motion of the neutral surface on the springback of U-shaped bending process is taken into account. The anisotropic nonlinear kinematic hardening model (ANK) is used to consider the impact of complex deformation, including stretching, bending and reverse bending. This model is able to investigate the Bauschinger effect, transient behavior and permanent softening. This model is used for the Numisheet2011 benchmark U-shaped bending problem. The effect of the sheet holder force, the coefficient of friction, thickness, material anisotropy, and hardening parameters on the sheet springback is studied. It can be seen that analytical model which presented in this paper has desirable accuracy in the springback prediction, and results are close to experimental data.

**Keywords** Springback · Bauschinger effect · Advanced high-strength steels · U-shaped bending process

✉ Asghar. Zajkani
zajkani@eng.ikiu.ac.ir

[1] Department of Mechanical Engineering, Imam Khomeini International University, Qazvin, Iran

## 1 Introduction

In forming process of sheet metals, undesired deformations caused by the release of elastic stress are serious problem which must be resolved in the optimization process. Materials with higher strength and lower modulus of elasticity have greater springback. For example, advanced high-strength steels (AHHS) have more springback compared to conventional steels because of higher strength. U-shaped bending processes are used in the production of components such as channels, beams, and frames. In this process, sheet metals experience complex deformation, including stretch-bending, stretch-unbending operation, and reverse bending. Therefore, after unloading in addition to the springback, the curvature of the side walls will be seen. Various methods, including analytical [1–4], semi-analytical methods [5–7], and finite element method (FEM) [8–11] are used to predict springback of bending process. FEM is time-consuming in comparison with the analytical methods and is sensitive to numerical parameters such as type and size of the elements.

Springback prediction accuracy increases when mechanical behavior is well described so the amount of springback depends on two main factors, namely, the stresses in the material before unloading and unloading modules [3, 10, 12, 13]. The mechanical behavior of materials in reverse loading due to reverse strain in the sheet metal forming process is highly regarded [13–15]. Figure 1 shows the flow stress curve on the outer surface of the sheet which initially bent around die arc and then straightened during the reverse bending. Four features can be seen in this curve that include Bauschinger effect (material yielding during reverse loading in less stress) [16], transient behavior (fast hardening in elastic-plastic transition zone against the forward loading) [17], permanent softening (existing a distance between the flow curves in forward and reverse loading) [17], and workhardening stagnation (stopping or slow the rate of work hardening) [18].

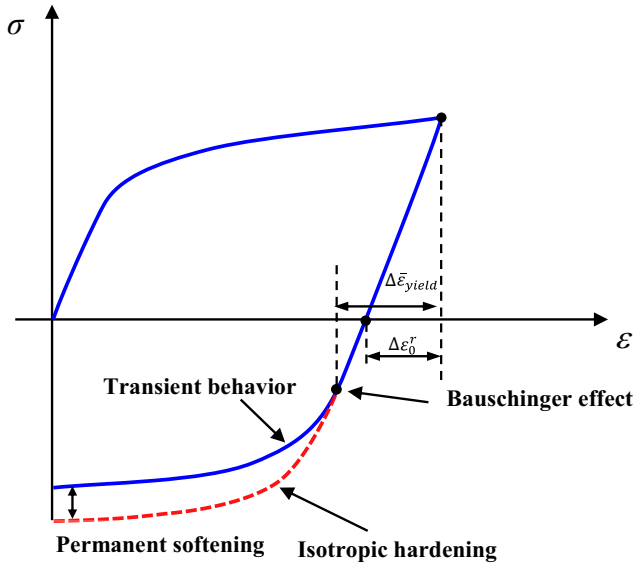


**Fig. 1** Unloading curve under reverse loading to show hardening behavior, including Bauschinger effect, transient behavior, and permanent softening

In past years, a few studies have been done for analytical springback prediction in comparison with the finite element method. Kagzi et al. [19] developed an analytical model for springback prediction in bending of bimetallic sheet based on Woo and Marshal constitutive equation and logarithmic strain. Yi et al. [20] proposed an analytical model based on residual differential strains between outer and inner surfaces after elastic recovery. In the case of V-bending process, Yang et al. [3] proposed an analytical model to predict the springback in air-bending of AHSS considering Young's modulus variation and with a piecewise hardening function. Zhang et al. [21] proposed a method for predicting sheet springback after V-bending Based on Hill's yielding criterion and plane strain condition. In the case of the double curvature forming process, Parsa et al. [22] presented an analytical model based on the moment–curvature relationships considering sheet thickness changes for predicting spring-back in double curved sheet metal forming process. Zhang and Lin [23] developed an analytical solution for springback prediction of sheet metals stamped by a rigid punch and an elastic die under plane-stress deformation. Xue et al. [24] established an analytical model based on the membrane theory of shells and an energy method after a double-curvature forming operation. In the case of U-bending process Pourboghrat [25] described a method for predicting springback in the two-dimensional draw bending operation using moment-curvature relationships. Zhang et al. [4] introduced an analytical model for predicting sheet springback after U-bending based on Hill48 yielding criterion, plane strain condition and kinematic, isotropic and combined hardening rules. Nanu and Brabie [2] presented a model for prediction of springback parameters during U stretch-bending process as a function of stresses distribution in the sheet thickness. Jiang and Dai [1] introduced an analytical model based on the isotropic hardening rule to predict U-bending springback and time-dependent springback behaviors for a HSLA steel plate.

The previous analytical models are not able to model the complex behavior of the material during the reversal loading such as the transient behavior and permanent softening. The analytical model presented here, implemented the anisotropic nonlinear kinematic hardening model (ANK), which can capture these complex behaviors of the material.

The main objective of the paper is to investigate the efficiency of a relatively complex nonlinear kinematic hardening model for a practical case study in metal forming process. A quantitative study of the material hardening parameters including Bauschinger effect, transient behavior, and permanent softening which influence on the springback is considered. For this purpose, an analytical model is presented based on a combined isotropic-kinematic hardening (ANK) model [26], Hill48 quadratic yielding criterion and plane strain condition. Furthermore, a Simpson type numerical integration method is used to obtain the springback parameters.

## 2 The relations between stress and strain in ANK hardening models

In the present model, the anisotropic nonlinear kinematic hardening model (ANK) is used to consider the effect of complex deformation that includes stretching, bending and unbending on the springback of U-shaped bending process. This hardening model is able to consider the Bauschinger effect, permanent softening and transient behavior during the forming process. As shown in Fig. 1, the flow stress during the forward uni-axial loading can be calculated as follows [26]:

$$\overline{\sigma}_{\text{forward}} = \sigma_{\circ} + R_{iso} + \alpha_{ANK}^{f} \tag{1}$$

where $\sigma_{\circ}$ is the initial yield stress and $R_{iso}$ is related to isotropic hardening and can be calculated by the following equation:

$$R_{iso} = Q\left(1-e^{-b\overline{\varepsilon}^{p}}\right)-\frac{C_1}{\gamma_1}\left(1-e^{-\gamma_1\overline{\varepsilon}^{p}}\right) \tag{2}$$

Also, $\alpha_{ANK}^{f}$ is the only nonzero component of the backstress tensor during uniaxial loading and its relation is as follows:

$$\alpha_{ANK}^{f} = \frac{C_1}{\gamma_1}\left(1-e^{-\gamma_1\overline{\varepsilon}^{p}}\right) + C_2\overline{\varepsilon}^{p} \tag{3}$$

In the above equations, $\overline{\varepsilon}^{p}$ is the equivalent plastic strain and $C_1$, $\gamma_1$, $C_2$, $Q$ and b are the material hardening parameters and their values are given in the Table 1 [13].

**Table 1** Material parameters of ANK hardening model for DP780

| b | $Q$ (MPa) | $\gamma_1$ | $C_2$ (MPa) | $C_1$ (MPa) | $\sigma_\circ$ (MPa) | $\bar{r}$ | $\bar{\varepsilon}_{lim}$ | $\nu$ |
|---|---|---|---|---|---|---|---|---|
| 29.9 | 402 | 44.1 | 124.2 | 10,154.1 | 527 | 0.781 | 0.198 | 0.3 |

The final relation between stress and equivalent plastic strain in forward uniaxial loading can be obtained by substituting Eqs. (2) and (3) into the Eq. (1) as follows:

$$\bar{\sigma}_{forward} = \sigma_\circ + Q\left(1-e^{-b\bar{\varepsilon}^p}\right) + C_2\bar{\varepsilon}^p \tag{4}$$

By considering $\bar{\varepsilon}^p_*$ as the equivalent plastic strain before reverse loading process, the following relationship can be obtained for the flow plastic stress during reverse loading:

$$\bar{\sigma}_{reverse} = -\sigma_\circ - R_{iso} + \alpha^r_{ANK} \text{ with } \bar{\varepsilon}^p > \bar{\varepsilon}^p_* \tag{5}$$

where $\alpha^r_{ANK}$ is the only nonzero components of back-stress tensor in the reverse loading stage and is calculated with the following equation:

$$\alpha^r_{ANK} = -\frac{C_1}{\gamma_1}\left(1-2e^{-\gamma_1\left(\bar{\varepsilon}^p-\bar{\varepsilon}^p_*\right)} + e^{-\gamma_1\bar{\varepsilon}^p}\right) - C_2\left(\bar{\varepsilon}^p - 2\bar{\varepsilon}^p_*\right) \text{ with } \bar{\varepsilon}^p > \bar{\varepsilon}^p_* \tag{6}$$

By substituting Eqs. (6) and (2) into Eq. (5), the following relation can be obtained for the plastic flow stress during reverse loading when $\bar{\varepsilon}^p > \bar{\varepsilon}^p_*$:

$$\bar{\sigma}_{reverse} = -\sigma_\circ - Q\left(1-e^{-b\bar{\varepsilon}^p}\right) - C_2\bar{\varepsilon}^p + \frac{2C_1}{\gamma_1}\left(e^{-\gamma_1\left(\bar{\varepsilon}^p-\bar{\varepsilon}^p_*\right)} - e^{-\gamma_1\bar{\varepsilon}^p}\right) + 2C_2\bar{\varepsilon}^p_* \tag{7}$$

## 3 Analysis of the stretch-bending process of the sheet

Deformation of the sheets at the edges of the punch and die can be considered as a stretch-bending process as shown in Fig. 2 with considering the following assumptions:

1. According to the Kirchhoff-Love plate theory, straight lines normal to the neutral surface remain straight during the stretch-bending process.
2. Sheet width in comparison with its thickness is large enough so the strain in the width direction $\varepsilon_z$ is zero.
3. Transverse stress $\sigma_r$ is neglected.
4. Volume conservation law during the stretch-bending process is considered.
5. During reverse bending process, the sheet thickness assumed to be unchanged and the tensile force in sidewall section is uniform and remains unchanged.

## 4 Thinning of sheet after the draw-bending process

The tangential and transverse engineering strain distribution in the thickness direction can be expressed by the following equations:

$$\varepsilon_\theta = \frac{r}{R_n} - 1 \tag{8}$$

$$\varepsilon_r = \frac{t}{t_0} - 1 \tag{9}$$

where $r$ and $R_n$ represent the curvature radius of the bending surface and neutral surface and $t_0$ and t are respectively the thickness before and after the stretch-bending process.

According to the volume conservation law and geometric relationship in Fig. 3, the following equation can be obtained [4]:

$$\frac{R_n}{R_m} = \frac{t}{t_0} \tag{10}$$

In the above equation, $R_m$ is the curvature radius of the sheet middle surface shown in Fig. 3 and calculated as follows:

$$R_m = R_i + \frac{t}{2} \tag{11}$$

In the above equation, $R_i$ is the curvature radius of the concave surface as shown in Fig. 3.

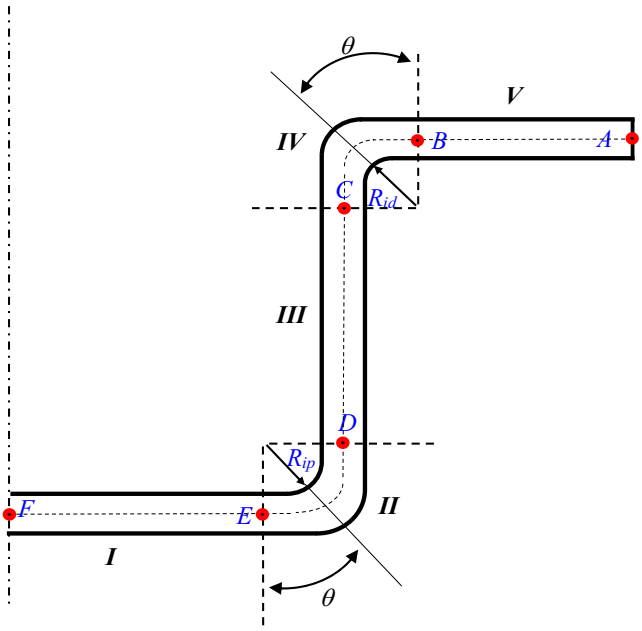


**Fig. 2** The schematic of the sheet U-bending part and different regions

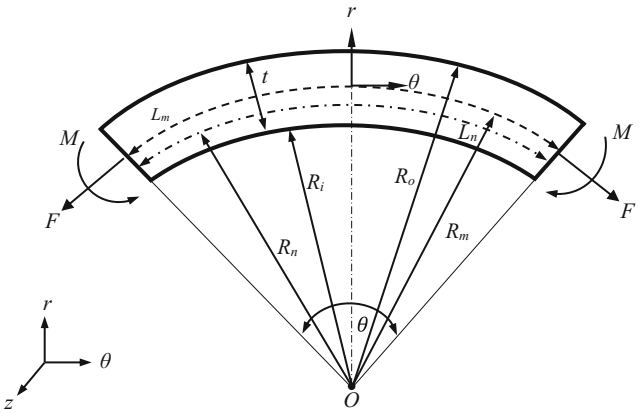


**Fig. 3** The schematic of sheet stretch-bending

## 5 Calculations after the draw-bending process

Using the Hill48 yielding criterion [27, 28] and assumption (3), the following equation can be obtained:

$$\overline{\sigma} = \frac{\sqrt{1+2\overline{r}}}{1+\overline{r}}|\sigma_\theta| = \frac{1}{G}|\sigma_\theta| \tag{12}$$

where $\sigma_\theta$ and $\overline{r}$ are respectively tangential stress and transverse anisotropy coefficient. The coefficient $G = (1+\overline{r})/\sqrt{1+2\overline{r}}$ is related to the transverse anisotropy in the plane strain condition. The transverse anisotropy coefficient is given in Table 1.

Also the equivalent strain can be expressed as follows:

$$\overline{\varepsilon}^p = G\,|\varepsilon_\theta| \tag{13}$$

Considering $R_o$ as the curvature radius of the convex surfaces and according to the Eqs. (4), (8), (12) and (13), the tangential stress distribution in the thickness direction ($\sigma_\theta$) can be expressed by the following equations:

$$\sigma_\theta = \begin{cases} G\left(\sigma_\circ + Q\left(1-e^{-Gb\left(\frac{r}{R_n}-1\right)}\right) + GC_2\left(\frac{r}{R_n}-1\right)\right) & R_n + c \le r \le R_o \\ \frac{E}{1-\nu^2}\varepsilon_\theta = E_1\frac{r-R_n}{R_n} & R_n - c \le r \le R_n + c \\ -G\left(\sigma_\circ + Q\left(1-e^{Gb\left(\frac{r}{R_n}-1\right)}\right) - GC_2\left(\frac{r}{R_n}-1\right)\right) & R_i \le r \le R_n - c \end{cases} \tag{14}$$

where $c$ is half the thickness of the elastic region and is expressed by the following equation:

$$c = \frac{G\sigma_\circ R_n}{E_1} \tag{15}$$

In addition, $E_1 = E/(1-\nu^2)$ is the Young's modulus in plane strain condition and $\nu$ is the Poisson's ratio.

According to Fig. 4, the tangential stress in middle surface ($R_m$) is equal to the stress produced by tensile force ($F = \sigma_{m\theta} t$) which is calculated by the following equation:

$$F = \begin{cases} G\left(\sigma_\circ + Q\left(1-e^{-Gb\left(\frac{R_m}{R_n}-1\right)}\right) + GC_2\left(\frac{R_m}{R_n}-1\right)\right)t & R_n + c \le R_m \le R_o \\ E_1\frac{R_m - R_n}{R_n}t & R_n \le R_m \le R_n + c \end{cases} \tag{16}$$

By substituting Eq. 10 into Eq. 16 have:

$$F = \begin{cases} G\left(\sigma_\circ + Q\left(1-e^{-Gb\left(\frac{t_0}{t}-1\right)}\right) + GC_2\left(\frac{t_0}{t}-1\right)\right)t & R_n + c \le R_m \le R_o \\ E_1\frac{t_0 - t}{t}t = E_1(t_0 - t) & R_n \le R_m \le R_n + c \end{cases} \tag{17}$$

The thickness of the sheet after stretch-bending process can be determined by using Eq. (17). Moreover, the radius of the neutral surface, the tangential stress, and strain distribution are obtained by using Eqs. (8), (10) and (14). Finally, the bending moment can be calculated using the following equation:

$$M_j = M_j^e + M_j^p, (j = II, IV) \tag{18}$$

where $M_j^e$ and $M_j^p$ are the respectively elastic and plastic moments of j-th section and can be obtained by following equations:

$$M_j^e = \int_{R_{nj}-C_j}^{R_{nj}+C_j} \left(\sigma_{\theta j} - \sigma_{m\theta j}\right)\left(r - R_{mj}\right)dr \tag{19}$$

$$M_j^p = \int_{R_{ij}}^{R_{nj}-c_j} \left(\sigma_{\theta j} - \sigma_{m\theta j}\right)\left(r - R_{mj}\right)dr + \int_{R_{nj}+c_j}^{R_{oj}} \left(\sigma_{\theta j} - \sigma_{m\theta j}\right)\left(r - R_{mj}\right)dr \tag{20}$$

### 5.1 The sheet reverse stretch-bending process

The sheet is stretched firstly under a tensile force applied by the punch and then bent around the die radius. Finally, it will be straight because of separation from the contact surface. During the reverse bending process, a tensile force is uniformly distributed. Because of the complex deformation history, the tangential stress and bending moments are dependent on the material hardening law.

According to assumption (5), the following relationship can be obtained for the curvature radius of the sheet in punch and the die coordinates (shown in Fig. 5):

$$r_p + r_d = R_{ip} + R_{id} + t_{sw} \tag{21}$$

In the above equation, $t_{sw}$ is the sidewall thickness, which is equal to the thickness at the end of the bending process around of die corner. The subscripts $p$ or $d$ are used in continues to show which coordinate (punch or die) is used to calculate the sheet parameters. Thus, $r_d$ and $r_p$ are respectively the curvature radiuses of the sheet in their coordinates. Moreover, $R_{id}$ and $R_{ip}$ are the radius of the die and punch corner.

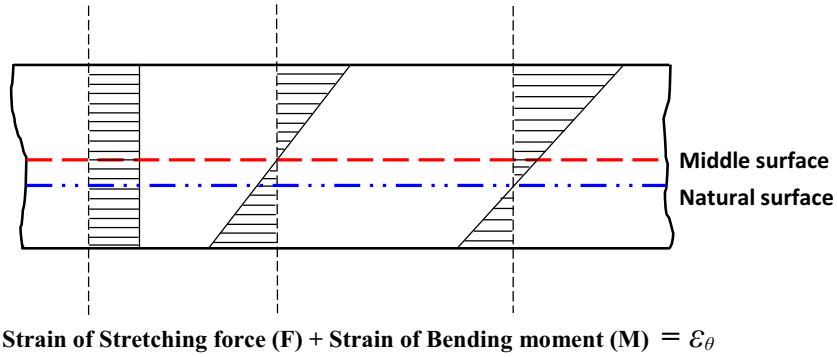


**Fig. 4** Scheme of stress distribution in sheet thickness during the stretch-bending process

The equivalent plastic strain caused by bending around the die corner during the forward loading can be calculated based on Eqs. (8) and (21) as follows:

$$\bar{\varepsilon}_d^p = |G\varepsilon_{\theta d}| = \left| G\left(\frac{r_d}{R_{nd}} - 1\right) \right| \tag{22}$$

Also, the equivalent strain after the reverse loading caused by bending around the punch corner can be expressed as follows:

$$\bar{\varepsilon}_p = |G\varepsilon_{\theta p}| = \left| -G\left(\frac{r_d}{R_{nd}} - 1\right) \right| \tag{23}$$

Considering $\bar{\varepsilon}_r^p$ as the equivalent plastic strain after the reverse loading stage, the following equations can be established:

$$\bar{\varepsilon}_r^p = \bar{\varepsilon}_p - \Delta\bar{\varepsilon}_{\text{yield}} + \bar{\varepsilon}_d^p \tag{24}$$

In Eq. (24), $\Delta\bar{\varepsilon}_{\text{yield}}$ is equal to the equivalent strain change in the reverse loading stage, where the flow stress reaches the yield stress (as shown in Fig. 1). Since during the reverse loading, yield occurs whenever $\bar{\varepsilon}_r^p = \bar{\varepsilon}_d^p$ and according to the Eqs. (4), (7) and (22), $\Delta\bar{\varepsilon}_{\text{yield}}$ can be calculated as:

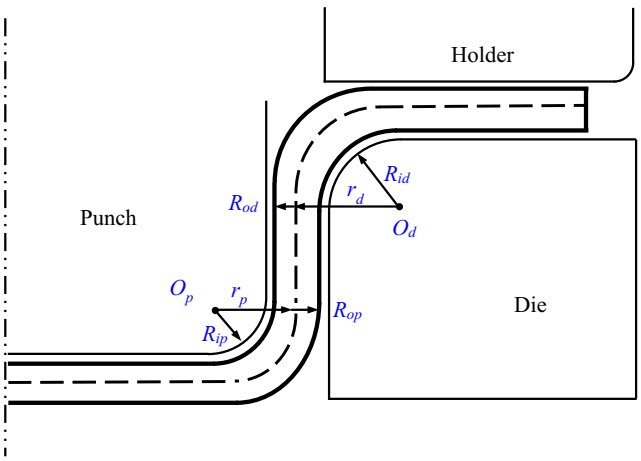


**Fig. 5** Scheme of relation between blank parameters in the die and punch coordinates for sidewall section

$$\Delta\bar{\varepsilon}_{\text{yield}} = \frac{2G\left[\sigma_\circ + Q\left(1 - e^{-b\bar{\varepsilon}_d^p}\right) - \frac{C_1}{\gamma_1}\left(1 - e^{-\gamma_1\bar{\varepsilon}_d^p}\right)\right]}{E_1} \tag{25}$$

In addition, $\Delta\varepsilon_0^r$ is equal to the strain which flow stress reaches to zero during the unloading process as shown in Fig. 1. According to the Eqs. (4) and (22), it can be calculated by the following equation:

$$\Delta\varepsilon_0^r = \frac{\sigma_\circ + Q\left(1 - e^{-b\bar{\varepsilon}_d^p}\right) + C_2\bar{\varepsilon}_d^p}{E_1} \tag{26}$$

Moreover, according to the Eqs. (7), (22), and 24, the tangential plastic stress in reverse loading ($\sigma_\theta^r$) in sidewall section can be calculated by following equations:

$$\sigma_\theta^r = G\left[\sigma_\circ + Q\left(1 - e^{-b\bar{\varepsilon}_r^p}\right) + C_2\bar{\varepsilon}_r^p - \frac{2C_1}{\gamma_1}\left(e^{-\gamma_1\left(\bar{\varepsilon}_r^p - \bar{\varepsilon}_d^p\right)} - e^{-\gamma_1\bar{\varepsilon}_r^p}\right) - 2C_2\bar{\varepsilon}_d^p\right] \tag{27}$$

The thickness of the sheet is divided into three sub-intervals in order to calculate the tangential stress in the reverse loading process as follows:

(1) Sub-interval (a): $R_{id} < r_d < R_{nd} - c$

I. If $R_{nd} - c > R_{\text{yield}}^{rt}$:

$$\sigma_\theta^{sw} = \begin{cases} \sigma_\theta^r & R_{ip} < r_d < R_{\text{yield}}^{rt} \\ E_1\left(\varepsilon_{\theta p} - \Delta\varepsilon_0^r\right) & R_{\text{yield}}^{rt} < r_d < R_{nd} - c \end{cases} \tag{28}$$

II. If $R_{nd} - c < R_{\text{yield}}^{rt}$:

$$\sigma_\theta^{sw} = \sigma_\theta^r \quad R_{id} < r_d < R_{nd} - c \tag{29}$$

In above equations, $R_{\text{yield}}^{rt}$ is the radius of curvatures where yield occurs in the plastic region during the reverse tensile loading process. According to the Eqs. (23) and (25), it can be obtained by solving the following equation:

$$\left|G\left(\frac{r_d}{R_{nd}}-1\right)\right| = \Delta\bar{\varepsilon}_{\text{yield}} \tag{30}$$

(2) Sub-interval (b): $R_{nd}-c<r_d<R_{nd}+c$

$$\sigma_\theta^{sw} = 0 \quad R_{nd}-c < r_d < R_{nd}+c \tag{31}$$

(3) Sub-interval (c): $R_{nd}+c<r_d<R_{od}$

I. If $R_{\text{yield}}^{rc} > R_{nd}+c$:

$$\sigma_\theta^{sw} = \begin{cases} E_1\left(\varepsilon_{\theta p}+\Delta\varepsilon_0^r\right) & R_{nd}+c < r_d < R_{\text{yield}}^{rc} \\ -\sigma_\theta^r & R_{\text{yield}}^{rc} < r_d < R_{od} \end{cases} \tag{32}$$

II. If $R_{\text{yield}}^{rc} < R_{nd}+c$:

$$\sigma_\theta^{sw} = \sigma_\theta^r \quad R_{nd}+c < r_d < R_{od} \tag{33}$$

In the above equations, $R_{\text{yield}}^{rc}$ is the radius of curvatures which yield occurs in the plastic region during the reversed compressive loading process and it can be calculated by solving the Eq. (30).

According to the assumption (5) during the reverse loading process, the thickness of the sheet is assumed to be unchanged. Thus, the middle surface stress is the same as before. According to Eqs. (30–35), the side wall section bending moment at point C (see Fig. 2) can be expressed as follows:

$$M_C = \int_{R_{id}}^{R_{od}} \left(\sigma_\theta^{sw}-\sigma_{m\theta}\right)\left(r_d-R_{md}\right)dr_d \tag{34}$$

The integral of Eq. (34) cannot be integrated analytically; thus, a Simpson type numerical integration method is used for the purpose.

## 6 Analysis U-shaped bending of sheet

Deformation in U-shaped bending process can be divided into five regions as shown in Fig. 2. The tensile force and bending moment that act on each region are shown in Fig. 6. Regions I and V are straight and are in contact with straight edges of punch and die.

Although in reality, these regions should be curved, but to simplicity, they are assumed to be straight due to the neglecting bending moment applied to the two parts. Regions II and IV are under tension-bending around the corners of punch and die. Region III is free and experiences the complex deformation history. The region IV, is bent firstly around the die corner and then be straight converted to the side wall. Due to the bending moment applied to region III, this region should have a curvature, but considering that the space between the die and punch is small compared to the punch stroke this region during the forming process straight assumed. However, after unloading the sheets in this region due to spring-back has rather a large curvature.

## 7 Calculation of tensile force in various parts of the sheet

In order to calculate the force acting on the region IV at each cross-section $\theta$, we use the following Eq. [4]:

$$F_{IV} = \mu_d P_{bh} e^{\mu_d \theta} \tag{35}$$

In the above equation, $\mu_d$ and $P_{bh}$ are the die friction coefficient and the blank-holding force, respectively. This equation indicates that the stretching force of the sheet in the die corner increases to reach to maximum value at point C:

$$F_C = \mu_d P_{bh} e^{\mu_d \varnothing} \tag{36}$$

In above equation, $\varphi$ is the total curvature angle of the die and punch. The amount of tensile force at each cross-section $\theta$ in region II is calculated using the following equation:

$$F_{II} = F_D e^{\mu_p(\theta-\varnothing)} \tag{37}$$

In the above equation, $\mu_p$ is the punch friction coefficient. This equation shows that the tensile force in the region II at cross-section E reaches its minimum value as follows:

$$F_E = F_D e^{-\mu_p \varnothing} \tag{38}$$

Because the region III is unsupported without external force, the following relation is established:

$$F_D = F_C \tag{39}$$

## 8 Calculation of sheet springback after U-shaped bending

The nonuniform distribution of stress in the cross section of the sheet during the forming process leads to create deformation and spring back during unloading. The sheet U-shaped bending springback occurs in the regions II, III, and IV, while regions I and V remain straight before and after unloading. It can be assumed that the springback in different regions is equal to the deformation of a reverse bending moment $-M(\theta)$. The spring-back angle in the regions II and IV can be calculated with the following equation:

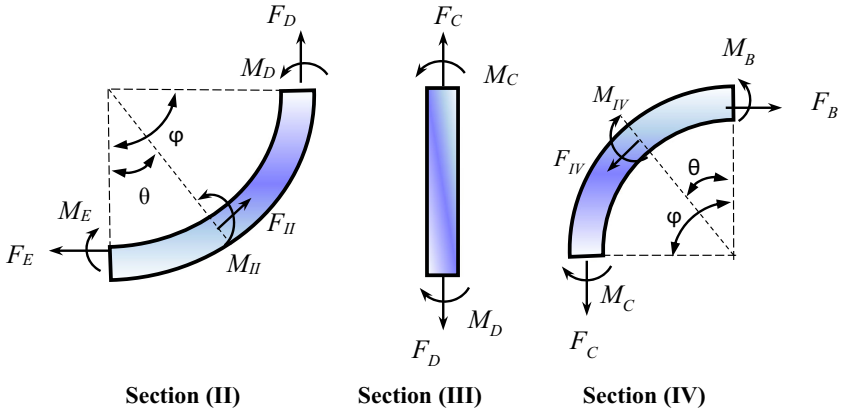


**Fig. 6** Schematic of loading and momentum for different regions of sheet

$$\Delta\theta = \int_0^{\varphi} \frac{M(\theta)}{E_1 I} R_m d\theta \tag{40}$$

Since the sheet is assumed to be straight in the region III, the angle change in this region can be obtained by the following equation:

$$\Delta\theta_{sw} = \frac{M_C L}{E_1 I} \tag{41}$$

Here, $I = t^3/12$ is the bending moment of inertia per unit width and $L$ is the length of the sidewall section. Also, for calculating the sidewall curvature radius, the following equation is used:

$$\frac{1}{\rho_{sw}} = \frac{M_C}{E_1 I} \tag{42}$$

## 9 Calculation of critical sheet holder force

Bending capability of the sheet is determined by the ultimate strain. The increase of holding force reduces springback, but causes the sheet thinning and increasing the tensile strain. It is also possible that the strain on the outer surface of the sheet exceeds the ultimate strain and creates initial cracks outside the sheet. The minimum thickness of the sheet can be obtained using the following equation:

$$G\left(\frac{R_{od}}{R_{nd}} - 1\right) = \bar{\varepsilon}_{lim} \tag{43}$$

After the calculation, the critical thickness of the sheet using the above equation and substituting it in the Eq. (17) the following equation can be obtained:

$$F_{\lim} = Gb\left(\sigma_\circ + Q\left(1 - e^{-Gb\left(\frac{t_0}{t_{\lim}} - 1\right)}\right) + GC_2\left(\frac{t_0}{t_{\lim}} - 1\right)\right) t_{\lim} \tag{44}$$

Whenever the sheet stretch force is more than $F_{\lim}$, sheet will rupture. Tensile force can be determined by the blank holder force and the friction between the sheet and the tools. By comparing the tensile force in different regions of the sheet, it can be seen that tension in the region III is the greatest value. Maximum blank holder force can be obtained by replacing Eq. (44) into Eq. (36) as follows:

$$P_{bh\max} = \frac{F_{lim}}{\mu_d e^{\mu_d \varphi}} \tag{45}$$

## 10 Results and discussion

This analytical model can be used for the analysis of two-dimensional stretch-bending process proposed in the Numisheet2011 benchmark problem [29]. Since the side wall experience bending, unbending and the reverse bending, this problem is suitable to examine different hardening criteria in modeling material mechanical behavior under reverse loading.

$\theta_1$, $\theta_2$, $\rho_{sw}$ and $\Delta\theta_{sw}$ are springback parameters which are shown in Fig. 7. If suppose the springback angle of regions II and III and IV, respectively, are equal to $\Delta\theta_1$ and $\Delta\theta_{sw}$ and $\Delta\theta_2$, then angles $\theta_1$ and $\theta_2$ can be calculated with the following equation:

$$\theta_1 = 90^\circ + \Delta\theta_1 + \frac{\Delta\theta_{sw}}{2} \tag{46}$$

$$\theta_2 = 90^\circ + \Delta\theta_2 - \frac{\Delta\theta_{sw}}{2} \tag{47}$$

The geometry and dimensions of the U-shaped stretch-bending problem have been reported by a schematic of Numisheet2011 benchmark problem shown in Fig. 8.

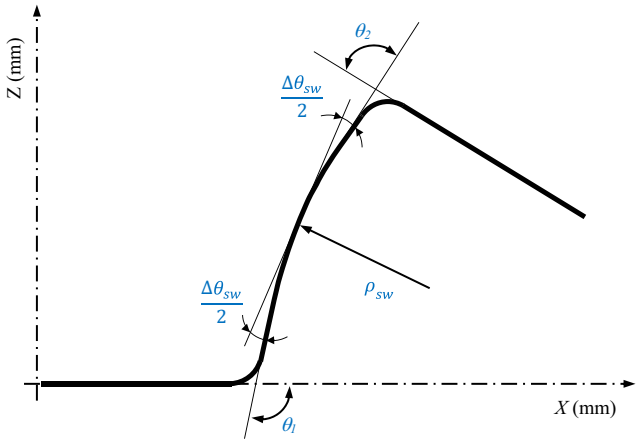


**Fig. 7** Schematic for springback measurement method

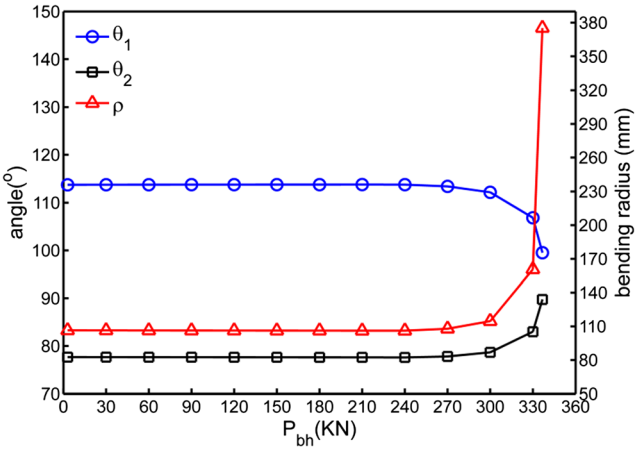


**Fig. 9** Influence of the blank holding force ($P_{bh}$) on the predicted springback parameters

The dual-phase DP780 steel sheet with a thickness of 1.4 mm is used in this test. Rectangular samples without pre-strain have been used with a width of 30 and 360-mm length [29]. During the forming process, the blank-holding force is equal to 2.94 KN. Punch speed is equal to 1 mm/s, while the punch stroke after the first contact between the punch and the sheet is equal to 71.8 mm. The friction coefficient between the tools and sheet is equal to 0.1. According to Eq. (45), the maximum value of the blank-holding force is 336.83 KN. In the following, the obtained results with the present analytical model are investigated to obtain the relation between the predicted springback parameters and geometrical and mechanical parameters of this problem.

Figure 9 shows the relation between springback parameters and blank holding force. It can be seen that increasing the blank-holding force up to 270 (KN) has no effect on the springback parameters.

The increase of the blank holding force decreases the springback angles, while it increases the curvature radius of the side wall. If the blank-holding force exceeds the critical value, it causes the rupture of the sheet.

Figure 10 illustrates the relation between the springback parameters and friction of die. It is similar to relation between the springback and blank holding force. If die friction exceeds the critical value, it causes the sheet rupture

Figure 11 displays the relation between punch friction and the springback angle ($\theta_1$). Punch friction change only causes the springback variation in region II. It can be seen that by increasing the punch friction the springback angle ($\theta_1$) increases. In this case, the blank holding force is assumed to be equal to 100 KN during the calculations

Figure 12 reflects the relation between the blank initial thickness and the springback parameters. The springback

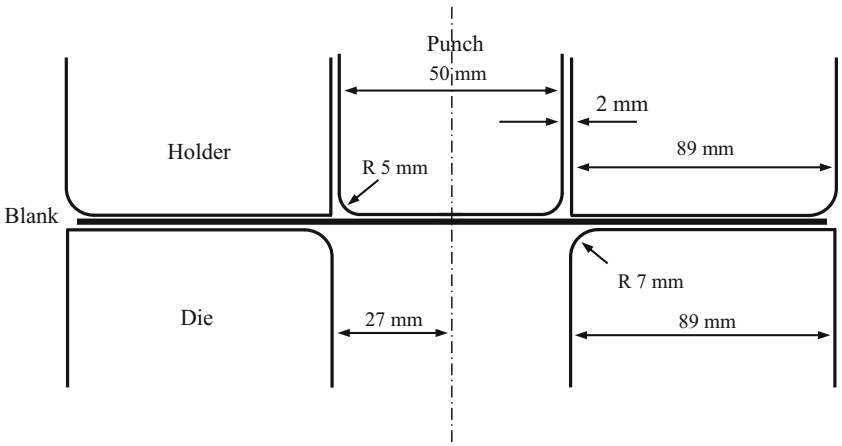


**Fig. 8** A schematic of Numisheet 2011 benchmark problem 2D draw bending

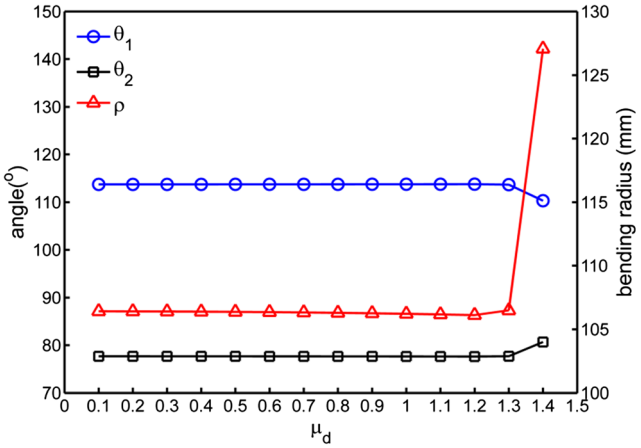


**Fig. 10** Effect of the die friction ($\mu_d$) coefficient on the predicted springback parameters

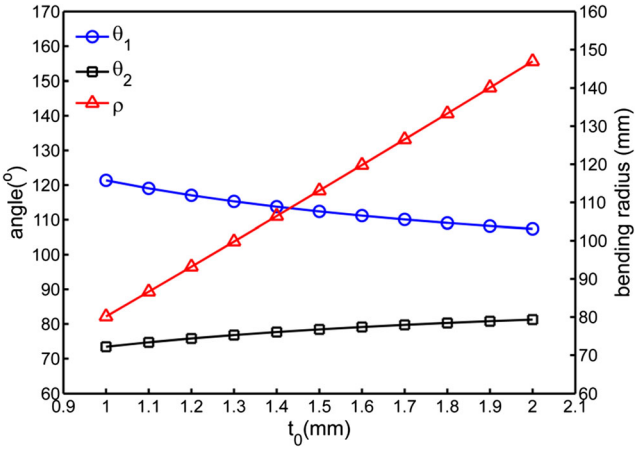


**Fig. 12** Effect of the sheet thickness on the predicted springback parameters

angles decrease with increasing initial thickness and curvature radius of the sidewall increase.

Figure 13 shows the effect of sheet anisotropy coefficient on the springback parameters. It can be seen that the springback angles increase with a small slope and curvature radius of sidewall decrease as anisotropy coefficient increase.

In order to validate the present analytical model introduced here, comparisons of the analytical predicted springback parameters with FEM and experimental results (Exp) are illustrated in Fig. 14. The finite element result obtained by Zang et al. [13] is based on the isotropic hardening (IH), anisotropic nonlinear kinematic hardening model (ANK), Yld2000-2d yielding criterion, and constant unloading modulus. All geometrical and mechanical parameters are the same with the Numisheet2011 benchmark problem [13]. It can be seen that all predicted springback parameters are close to the experimental results except the side wall curvature radius.

Hardening parameters $C_1$, $C_2$ , and $\gamma_1$ are related to the hardening behavior of materials, including Bauschinger effect, transient behavior, and permanent softening. Thus, the effect of hardening behavior on spring back can be investigated by changing these parameters.

Figure 15 illustrates the relation between $\gamma_1$ and springback parameters. The variation in springback parameters tends to decrease as $\gamma_1$ increase while the variation of springback parameters tends to increase as $\gamma_1$ decreases. As well as curvature radius in comparison with springback angles have greater variations. This means that hardening behavior under strain reversal has a more significant

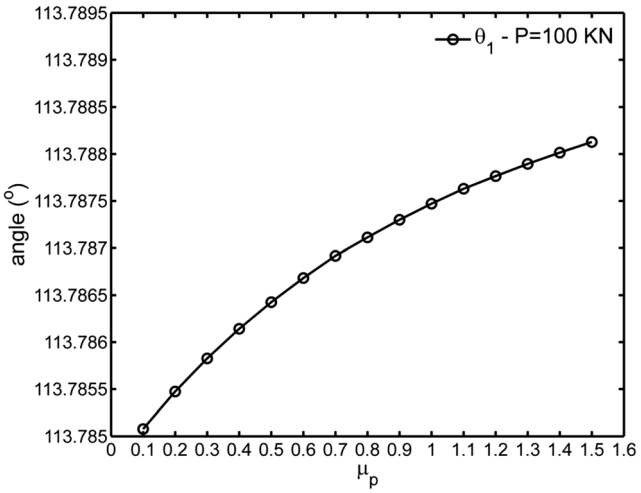


**Fig. 11** Effect of the punch friction ($\mu_p$) coefficient on the springback prediction

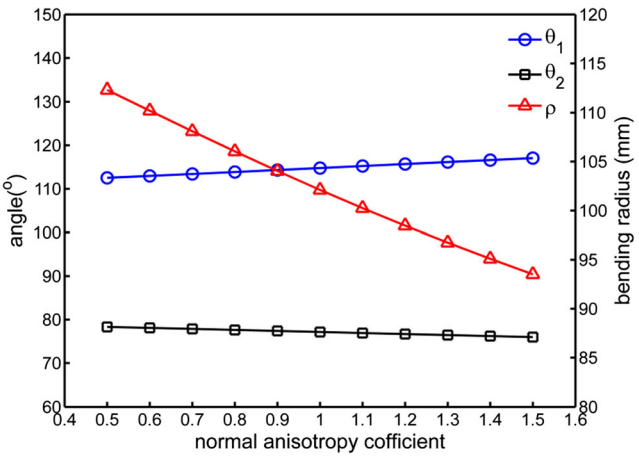


**Fig. 13** Effect of the anisotropy coefficient on the predicted springback parameters

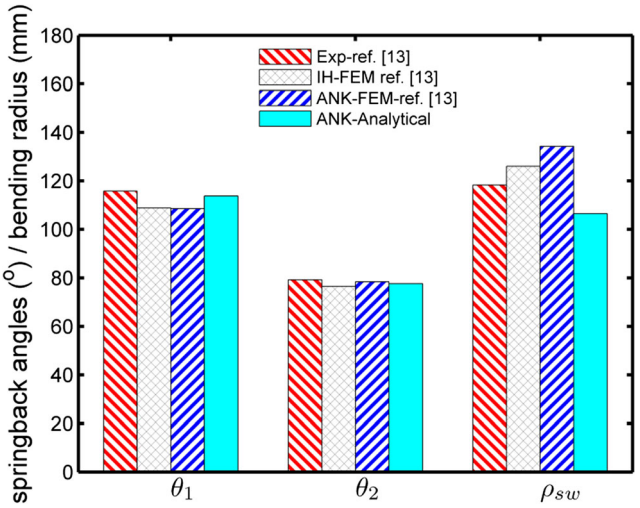


**Fig. 14** Several experimental and theoretical predictions of the springback parameters based on FEM method [13, 30] and analytical method

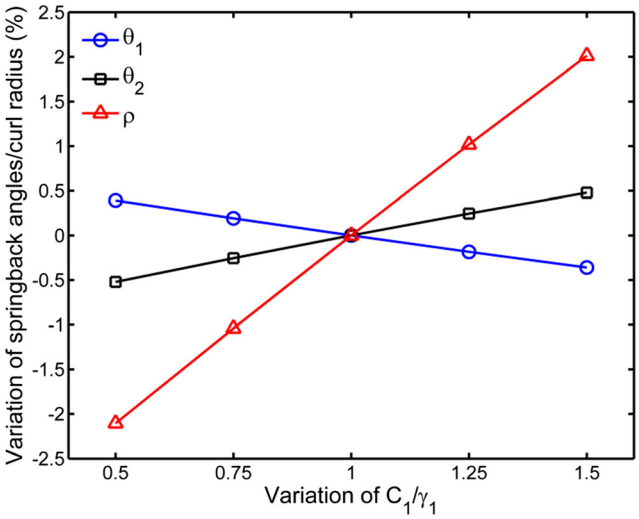


**Fig. 16** Influence of $C_1/\gamma_1$ in the springback angles prediction

influence since material inside the wall experience complex deformation including loading-unloading and reverse loading.

Figure 16 displays the effect of $C_1/\gamma_1$ variation on the predicted springback parameters. Comparing with the effect of $\gamma_1$, $C_1$ has less effect on the amount of predicted springback parameters and almost linear relationship is resulted between $C_1$ and variation of springback parameters. The variations of curvature radius of side wall are noticeable

Figure 17 reflects the relation between $C_2$ and predicted springback parameters. It can be seen there is a linear relationship between $C_2$ and springback parameters and the effect of parameter $C_2$ variation on the springback parameters is less than $C_1$ and $\gamma_1$.

## 11 Conclusion

In this paper, a new analytical model based on Hill48 yielding criterion and plane strain conditions of hardening has been introduced to predict the springback phenomenon in the U-shaped bending process. The model is used to solve the Numisheet2011 benchmark problem, and the results are in good agreement with the experimental data. The ANK hardening model is used which has the ability to take into account the hardening

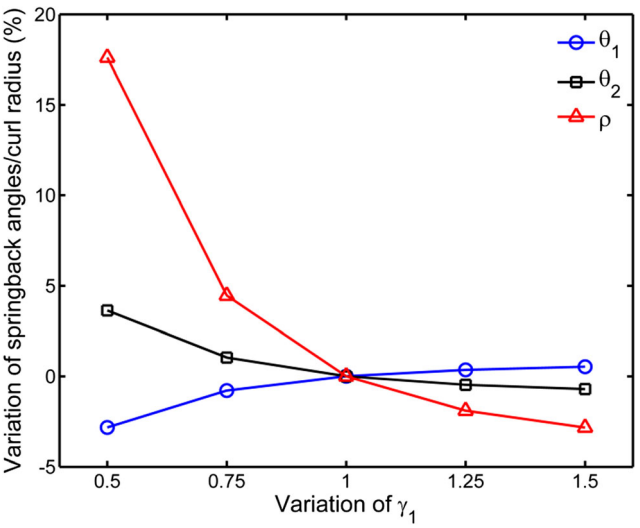


**Fig. 15** Influence of $\gamma_1$ in the springback angles prediction

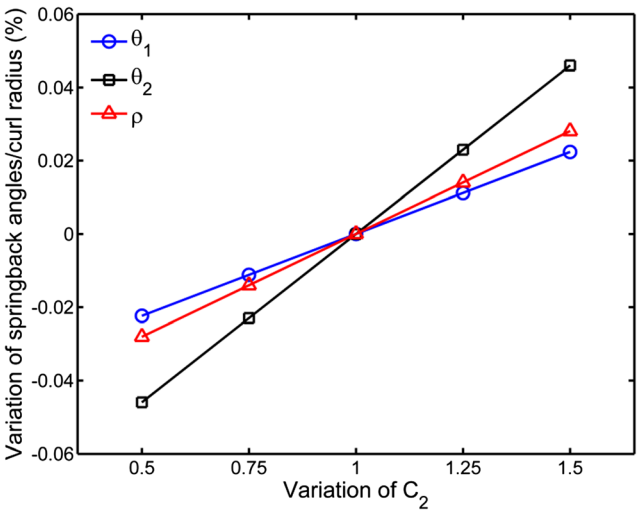


**Fig. 17** Influence of $C_2$ in the springback angles prediction

behavior of the material such as Bauschinger effect, permanent softening and transient behavior in the reverse loading process, simultaneously. The results obtained from this model are compared with results of FEM simulation, and it can be seen that present analytical results in some cases are closer to the experimental data in comparison with FEM simulation.

The effect of hardening parameters including $C_1$, $C_2$, and $\gamma_1$ and geometrical parameters on springback prediction is investigated. It can be seen that with increasing $\gamma_1$ and $C_2$, springback angle increases while with increasing $C_1$ springback angles decrease. Also with increasing $\gamma_1$, the curvature radius of side wall decreases while with increasing $C_1$ and $C_2$ the curvature radius of the side wall increases. The increase of the blank-holding force and friction between the die and sheet causes declining springback. The punch friction only affects the springback angle in region II and with increasing the punch friction the springback angle ascends. It can be seen that springback decreases as the initial thickness of blank increases while it increases with increasing anisotropy of sheet.

This work can be regarded as a benchmark model to consider the efficiency of similar constitutive equations for relatively complex hardening models, independence of eventual numerical errors.

## References


1. Jiang H-J, Dai H-L (2015) A novel model to predict U-bending springback and time-dependent springback for a HSLA steel plate. Int J Adv Manuf Technol 81:1055–1066
2. Nanu N, Brabie G (2012) Analytical model for prediction of springback parameters in the case of U stretch-bending process as a function of stresses distribution in the sheet thickness. Int J Mech Sci 64:11–21
3. Yang X, Choi C, Sever NK, Altan T (2016) Prediction of springback in air-bending of advanced high strength steel (DP780) considering Young′ s modulus variation and with a piecewise hardening function. Int J Mech Sci 105:266–272
4. Zhang D, Cui Z, Ruan X, Li Y (2007b) An analytical model for predicting springback and side wall curl of sheet after U-bending. Comput Mater Sci 38:707–715
5. Le Quilliec G, Breitkopf P, Roelandt J-M, Juillard P (2014) Semi-analytical approach for plane strain sheet metal forming using a bending-under-tension numerical model. Int J Mater Form 7:221–232
6. Lee M-G, Kim D, Wagoner RH, Chung K (2007) Semi-analytic hybrid method to predict springback in the 2D draw bend test. J Appl Mech 74:1264–1275
7. Panthi SK, Ramakrishnan N (2011) Semi analytical modeling of springback in arc bending and effect of forming load. Trans Nonferrous Met Soc China 21:2276–2284
8. Chongthairungruang B, Uthaisangsuk V, Suranuntchai S, Jirathearanat S (2012) Experimental and numerical investigation of springback effect for advanced high strength dual phase steel. Mater Des 39:318–328
9. Guo C, Chen J, Chen J, et al. (2010) Numerical simulation and experimental validation of distortional springback of advanced high-strength steel sheet metal forming. J Shanghai Jiaotong Univ 4:6
10. Kim H, Kimchi M (2011) Numerical modeling for springback predictions by considering the variations of elastic modulus in stamping advanced high-strength steels (AHSS). 8th Int Conf Work Numer Simul 3D seet Met Form Process (NUMISHEET 2011) 1159–1166
11. Zhang RY, Zhao GY, Guo ZH, Quan YP (2015) Effects of material parameters on springback of 5052 aluminium alloy sections with hat profile in rotary draw bending. Int J Adv Manuf Technol 80:1067–1075
12. Lee J, Lee J-Y, Barlat F, et al. (2013) Extension of quasi-plastic–elastic approach to incorporate complex plastic flow behavior—application to springback of advanced high-strength steels. Int J Plast 45:140–159
13. Zang S, Lee M, Kim JH (2013) Evaluating the significance of hardening behavior and unloading modulus under strain reversal in sheet springback prediction. Int J Mech Sci 77:194–204
14. Geng L, Shen Y, Wagoner RH (2002) Anisotropic hardening equations derived from reverse-bend testing. Int J Plast 18:743–767
15. Eggertsen P-A, Mattiasson K (2010) On constitutive modeling for springback analysis. Int J Mech Sci 52:804–818
16. Chun BK, Jinn JT, Lee JK (2002) Modeling the Bauschinger effect for sheet metals, part I: theory. Int J Plast 18:571–595
17. Gutierrez-Urrutia I, Del Valle JA, Zaefferer S, Raabe D (2010) Study of internal stresses in a TWIP steel analyzing transient and permanent softening during reverse shear tests. J Mater Sci 45: 6604–6610
18. Yoshida F, Uemori T (2002) A model of large-strain cyclic plasticity describing the Bauschinger effect and workhardening stagnation. Int J Plast 18:661–686
19. Kagzi SA, Gandhi AH, Dave HK, Raval HK (2016) An analytical model for bending and springback of bimetallic sheets. Mech Adv Mater Struct 23:80–88
20. Yi HK, Kim DW, Van Tyne CJ, Moon YH (2008) Analytical prediction of springback based on residual differential strain during sheet metal bending. Proc Inst Mech Eng Part C J Mech Eng Sci 222:117–129
21. Zhang D, Cui Z, Chen Z, Ruan X (2007a) An analytical model for predicting sheet springback after V-bending. J Zhejiang Univ Sci A 8:237–244
22. Parsa MH, Pishbin H, Kazemi M, others (2012) Investigating spring back phenomena in double curved sheet metals forming. Mater Des 41:326–337.
23. Zhang LC, Lin Z (1997) An analytical solution to springback of sheet metals stamped by a rigid punch and an elastic die. J Mater Process Technol 63:49–54
24. Xue P, Yu TX, Chu E (1999) Theoretical prediction of the springback of metal sheets after a double-curvature forming operation. J Mater Process Technol 89:65–71
25. Pourboghrat F, Chu E (1995) Springback in plane strain stretch/draw sheet forming. Int J Mech Sci 37:327–341
26. Zang SL, Guo C, Thuillier S, Lee MG (2011) A model of one-surface cyclic plasticity and its application to springback prediction. Int J Mech Sci 53:425–435
27. Wagoner RH (1980) Measurement and analysis of plane-strain work hardening. Metall Mater Trans A 11:165–175
28. Hill R (1998) The mathematical theory of plasticity. Oxford University press
29. Chung K, Kuwabara T, Verma RK, et al. (2011) Pre-strain effect on spring-back of 2-D Draw bending. Numisheet 2011, Benchmark 4
30. Lee J-Y, Lee J-W, Lee M-G, Barlat F (2012) An application of homogeneous anisotropic hardening to springback prediction in pre-strained U-draw/bending. Int J Solids Struct 49:3562–3572